

## Probable Interaction of Reduced Glutathione with NF- $\kappa$ B Family Proteins Trim down NF- $\kappa$ B Mediated Expression of MMP-9: An in Silico Analysis

Nitin Ghoshal<sup>1\*</sup>, Baphilinia J Myllemngap<sup>2</sup> and Atanu Bhattacharjee<sup>2</sup>

<sup>1</sup> Radiation Biology Laboratory, Inter-University Accelerator Centre, New Delhi, India

<sup>2</sup> Department of Biotechnology and Bioinformatics, North-Eastern Hill University, Shillong, India

\*Corresponding author's e-mail: ngbiotech@gmail.com

**ABSTRACT:** Tumor invasion and metastasis require increased expression of matrix metalloproteinases (MMPs). MMP family is involved in the degradation of extracellular matrix, and members of MMPs have been implicated in malignancy and metastasis. Recent data suggest that antioxidant treatment inhibits gelatinolytic activity. It has been shown that ROS activate gelatinase B (MMP-9) and antioxidants are able to limit ROS induced MMP activity. However, how oxidative stress regulates MMP expression is not yet fully understood. The promoter of MMP-9 is highly conserved and is shown to contain multiple functional elements, including nuclear factor- $\kappa$ B (NF- $\kappa$ B) and activator protein 1 (AP-1) element. NF- $\kappa$ B has been shown to regulate the expression of a number of genes, such as vascular endothelial growth factor and MMP-9, whose products are involved in tumorigenesis. MMP9 expression depends on the redox status of a cell in a NF- $\kappa$ B dependent manner. We, hereby, put forward that reduced glutathione (GSH) binds to the NF- $\kappa$ B activating kinases rendering it inactive for the phosphorylation of I $\kappa$ B, the event, which releases NF- $\kappa$ B for its nuclear transport. Thus at optimum concentration of GSH, NF- $\kappa$ B family could be a probable target for inhibiting MMP9 therefore checking metastasis.

**KEYWORDS:** Cancer, Glutathione, Matrix Metalloproteinases, Metastasis, NF- $\kappa$ B

ORIGINAL ARTICLE  
Received 12 Jan. 2014  
Accepted 15 Mar. 2014

### INTRODUCTION

The chain of events capable of uprooting the links to survival of human beings have become more complex, especially in cancer cases where number of deaths is expected to be approximately one million per year. Tumor invasion and metastasis require increased expression of matrix metalloproteinases (MMPs) [1]. MMP family is involved in the degradation of extracellular matrix and their role have also been implicated in malignancy and metastasis [1]. Recent data suggest that antioxidant treatment inhibits gelatinolytic activity [2, 3, and 4]. It has been shown that ROS activate gelatinase B (MMP-9) and antioxidants are able to limit ROS induced MMP activity [2]. However, how oxidative stress regulates MMP expression is not yet fully understood. Ionizing radiation acts through the induction of double strands break to DNA to induce elimination of cancerous cells via apoptosis. NF- $\kappa$ B and AP-1 are activated by DNA damaging agents and could be involved in cell cycle arrest and prevention of apoptosis to allow DNA repair [5, 6]. A decrease in the translocation of NF- $\kappa$ B subunits (p50 and p65) and AP-1 subunits (c-fos and Jun D) was noted in the cells that received the combined treatment of Ad-MMP9 (an inhibitor of MMP9) and radiation [7]. Cancer cells often develop radioresistance mechanisms in relation to DNA repair. By combining chemo and radiotherapy, radiation efficacy may be strengthened by inhibiting DNA repair and overcome resistance to apoptosis. NF- $\kappa$ B is turned on by DNA damaging agents and could be involved in cell cycle arrest and prevention of apoptosis, allowing DNA repair [5]. However, sustained NF- $\kappa$ B activation could permit cells with accumulated radiation induced DNA damage to escape elimination by apoptosis [8]. Indeed, high constitutive NF- $\kappa$ B activity prevents cancerous cells from apoptosis [9], resulting in a more aggressive potential seen in prostate cancer [10], malignant melanomas, Hodgkin's disease, breast cancer, leukemia, and cutaneous T-cell lymphoma cancer cell lines [11].

The promoter of MMP-9 is highly conserved and contains multiple functional elements, including nuclear factor- $\kappa$ B (NF- $\kappa$ B) and activator protein 1 (AP-1) element [12]. NF- $\kappa$ B has been shown to regulate the expression of innumerable genes, for example, vascular endothelial growth factor and MMP-9, whose products are implicated in tumorigenesis [13]. Several evidences indicate that the suppression of MMP-9 prevents invasion and metastasis [14]. MMP-9 has been considered to be an important factor in facilitating invasion and metastasis in pancreatic cancer [15]. Moreover, Muroso et al demonstrated that the invasiveness induced by Epstein-Barr virus latent membrane protein-1 is correlated with the induction of MMP-9 [16]. Thus, agents that inhibit the activation of NF- $\kappa$ B or MMP-9 may exhibit the therapeutic potential for the suppression of carcinogenesis and tumor metastasis [13, 17]. MMP9 expression may depend on the redox status of a cell in a NF- $\kappa$ B dependent manner. Therefore, thiol supplementation may also inhibit NF- $\kappa$ B activation thereby reducing MMP9 expression. This strategy has not been tested therapeutically, thus we accept the challenge and hereby, hypothesize, as illustrated in fig: 1(A), that reduced

glutathione (GSH) binds to the NF- $\kappa$ B activating kinases (i.e. IKK and GSK3) rendering it inactive for the phosphorylation of I $\kappa$ B, the event, which releases NF- $\kappa$ B for its nuclear transport. Besides, GSH even binds to the I $\kappa$ B-NF $\kappa$ B complex and shields the complex from getting phosphorylated by the NF- $\kappa$ B activating kinases.

## MATERIAL AND METHODS

**Structure retrieval:** The pdb structure of free GSH was not available, so it was created using “Chem3D Ultra 8.0” and the energy minimization was performed using “MM2” environment for obtaining the most stable structure. The pdb structures 1IKN, 3BRV, 3BRT, 1I09, 1L6J and 3MVM were retrieved from the RCSB PDB Protein Data Bank with the following details (i) 1IKN (NF- $\kappa$ B P65 subunit, NF- $\kappa$ B P50 D subunit, I- $\kappa$ B  $\alpha$ ) DOI: 10.2210/pdb1ikn/pdb (ii) 3BRV (Inhibitor of nuclear factor kappa-B kinase subunit beta, NF-kappa-B essential modulator) DOI:10.2210/pdb3brv/pdb (iii) 3BRT (Inhibitor of NF- $\kappa$ B kinase subunit  $\beta$ ,  $\alpha$  and NF- $\kappa$ B essential modulator) DOI: 10.2210/pdb3brt/pdb (iv) 1I09 (Glycogen synthase kinase 3  $\beta$ ) DOI: 10.2210/pdb1i09/pdb (v) 1L6J (Matrix metalloproteinase-9) DOI: 10.2210/pdb1l6j/pdb (vi) 3MVM (P38 Alpha Map Kinase complexed with pyrrolotriazine inhibitor 7V) DOI: 10.2210/pdb3mvm/pdb (used as positive control for docking score comparison).

**Protein-protein Interaction Studies:** The structural details of interactions of 1IKN, 1L6J, 1I09, 3BRT, 3BRV and 3MVM with GSH were elucidated by molecular docking experiments. Protein-protein interaction simulation (docking) experiments could not be performed using Rosetta Dock server (<http://rosettadock.graylab.jhu.edu>) since the docking protein must have minimum of 6 units and GSH is a tri-peptide. Therefore, we used Hex-6.3 software for surface docking simulations. In these docking calculations, each molecule is modeled using 3D expansions of real orthogonal spherical polar basis functions to encode both surface shape and electrostatic charge and potential distributions. All docking experiments were replicated 1000 times and best Etotal for the interaction was taken as a key parameter to evaluate the significance of interaction. E total was represented in terms of KJ/mol.

Gold suite 5.0 is used for verification of the results as this is fully licensed, besides it is rated as the best for molecular docking experiments [18]. The fitness score is taken as the negative of the sum of the component energy terms, so that larger fitness scores are better. Positive control is generated for comparison of docking score using the protein 3MVM (i.e. P38 Alpha Map Kinase complexed with pyrrolotriazine inhibitor 7V). This inhibitor is highly specific and presently being used in phase-II clinical trials for treatment of rheumatoid arthritis. This ligand is separated from P38  $\alpha$ -MAPK and re-docked using Gold suite v5.0 to generate fitness score to be used as a positive control for comparison to the test docks. Ramachandran Plots are generated using Procheck before docking and after docking to analyze any conformational change, if at all present.

**Visualization:** A 2D molecular display method has been added to MOE 2006 (Molecular Operating Environment), which is designed for viewing the active sites of protein:ligand complexes (Fig: 1). Residues are annotated with their 3-letter amino acid code, and their position classification. Hydrophobic residues are all colored with a green interior, whereas polar residues are colored in light purple. Hydrogen bonding interactions between the receptor and the ligand are drawn with an arrowhead to denote the direction of the hydrogen bond (i.e. the donor is at the base of the arrow, and the acceptor is at the head). The ligand is always drawn in a conventional 2D schematic form, with most of the hydrogen atoms either implied or subsumed into the atom label. Hydrogen atoms unambiguously involved in a hydrogen bond are sketched individually, and oriented toward the residues with which they interact.

**Binding Energy Calculation:** PEARLS (Program for Energetic Analysis of Ligand-Receptor Systems) [19], a Web-based software, for computing interaction energies of protein-ligand complexes from their 3D structures. The computed free energy for a number of PDB ligand-receptor complexes were studied and compared to experimental binding affinity. A substantial degree of correlation between the computed free energy and experimental binding affinity was found, which suggests that PEARLS may be useful in facilitating energetic analysis of ligand-protein complex and therefore being used in the present study.

## RESULTS

Vanillin (a component of vanilla) displays the “antioxidant activity” through the protection of membranes against photosensitization induced oxidative damage in rat liver mitochondria [20, 21]. It has been known to inhibit cell invasion and migration, suppress enzymatic activity of MMP-9 [22]. This triggered the idea whether GSH can mimic vanillin or not. But how the inhibition of dissociation of NF- $\kappa$ B from I- $\kappa$ B occurs in the presence of reduced glutathione, is still unanswered. There are two possible ways for GSH to accomplish this (i) it may bind to the ‘NF $\kappa$ B-I $\kappa$ B’ complex such that the phosphorylation sites are shielded (ii) it may bind to the kinases that phosphorylate I- $\kappa$ B e.g. IKK, CK2 etc. To unfold the mechanism it was important to know if GSH exhibits any affinity towards I $\kappa$ B-NF $\kappa$ B complex and its kinases. Pdb structure of GSH was produced using “Chem draw 3D ultra v8.0” and structures of I $\kappa$ B-NF $\kappa$ B complex, IKK, GSK3B, and MMP9 were retrieved from RCSB PDB Protein Data Bank. Surface docking study was done using Hex 6.3 software and verified by Gold suite 5.0.

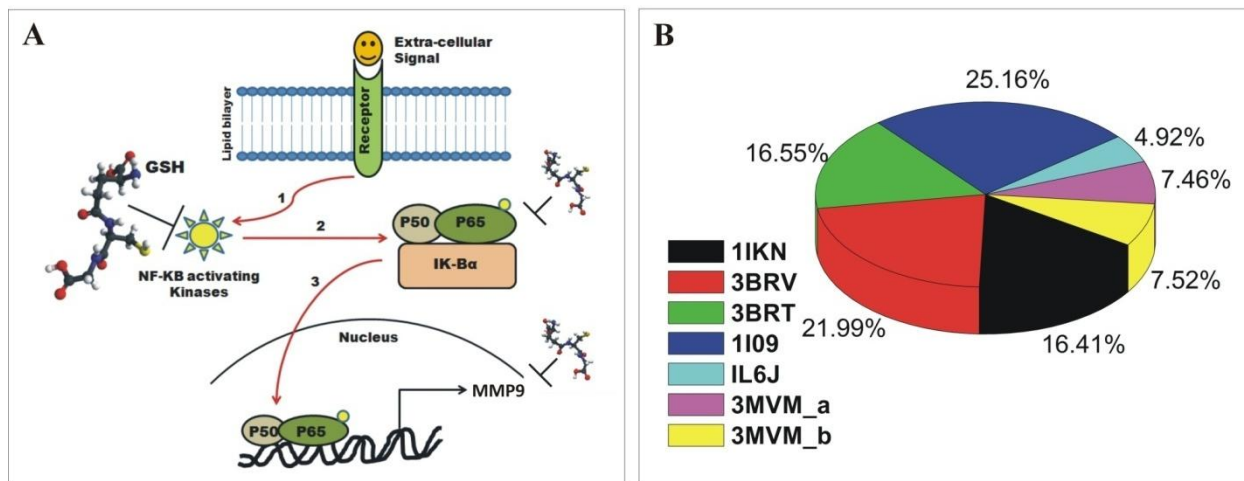


**Fig 1.** (A) Graphical concept of the hypotheses. (B) Percentage contribution in affinity towards GSH using HEX

**Fig:1 (A)** A graphical representation of the hypothesis showing the potential of GSH to block activation by inhibiting the phosphorylating ability of NAK (NF-κB activating kinases) and nuclear-translocation of NF-κB in addition to sequestration of MMP9. **(B)** GSH showed highest affinity towards the kinases as expressed in  $E_{total}$  values i.e.  $-1038.75 \text{ KJ.mol}^{-1}$  for GSK3β (1109) followed by NEMO/IKK (3BRV) with  $-908.03 \text{ KJ/mol}$ . It has relatively low affinity towards IκB-NFκB complex (11KN) i.e.  $-677.34 \text{ KJ/mol}$ , followed by  $-683.08 \text{ KJ/mol}$  for which NEMO/IKK (α, β) (3BRT) subunits and GSH interaction was found responsible. GSH even binds to the MMP9 protein (IL6J) as shown by docking experiment, yielding an  $E_{total}$  of  $-202.93 \text{ KJ/mol}$  which is though quite less in comparison to the kinases. The positive control  $E_{total}$  values for the two subunits of P38 MAPK complexed with inhibitor (3MVM\_a and b) are  $-307.94$  and  $-310.47$ . Comparing to the positive control the kinases show relatively more affinity towards GSH. The higher  $E_{total}$  value assures the probability of interaction in real time.

**Surprisingly, as in fig: 1(B)**, GSH showed very high affinity towards the kinases as expressed in  $E_{total}$  values i.e.  $-1038.75 \text{ KJ.mol}^{-1}$  for GSK3β followed by NEMO/IKK with  $-908.03 \text{ KJ/mol}$ . This indicates that there is high probability of GSH binding to the kinases and inhibiting their phosphorylation ability. Besides, it has relatively low affinity towards IκB-NFκB complex (i.e.  $-677.34 \text{ KJ/mol}$ ) suggesting some role in shielding the complex from active kinases, this followed by  $-683.08 \text{ KJ/mol}$  for which by NEMO/IKK (α, β) subunits accepted the responsibility. GSH even binds to the MMP9 protein as shown by docking experiment, yielding an  $E_{total}$  of  $-202.93 \text{ KJ/mol}$  which is though quite less in comparison to the kinases. The positive control  $E_{total}$  values for the two subunits of P38 MAPK complexed with inhibitor are  $-307.94$  and  $-310.47$  respectively. Comparing to the positive control in fig: 1(B) the kinases show relatively more affinity towards GSH. The higher  $E_{total}$  value assures the probability of interaction in real time.

**In Table: 1**, using Gold suite 5.0, the fitness score is maximum i.e. 54.49 for 1L6J (MMP9). The thiol group of GSH shows affinity with oxygen atom of Leu397 on MMP9. The fitness score for GSH and 3BRV (NEMO/Iκk associated domain) is found to be 54.36 with thiol group reaction at Ser68. Significant docking score of 50.42 is found to be associated with 11KN (IκBα/NF-κB complex). With GSK3 i.e. 1109 the obtained score is 49.37 along with thiol group interaction at Cys218 and Asp260. The NEMO/Iκk association domain (i.e. 3BRT) has shown the lowest fitness score of 47.86 but in addition has pronounced reaction of Sulfur of Cys in GSH at two places i.e. Gln730, Glu89 of 3BRT. All the scores are comparable to the fitness score of 58.06 and 60.42 of the positive control which are not significantly lower indicating probable interaction. The number of hydrogen bonds are more in the test docks than in the control. The interaction pattern in the positive control indicates that more the sharing of hydrogen from the Nitrogen atom, more the fitness score and hence the strength of inhibition of the ligand. The bond length is considered better if it is more than 2.0 nm. The bond length is more than 2.0 nm in all the cases of interaction which strengthens the hypothesis. Even in the interaction of GSH with 1L6J (i.e. MMP9) the probable glutathionylation at oxygen atom of Leu397 the bond length is 3.09 besides, there is bond sharing with N1 of GSH at oxygen atom of Met422 having a bond length of 2.548. This indicates direct inhibition of MMP9 by GSH. The interaction of the probable hydrogen bonds are illustrated in **fig: 2** using MOE v6.0.

**Fig: 2** 2D molecular display method has been employed using MOE 2006 (*Molecular Operating Environment*), which is designed for viewing the active sites of protein: ligand complexes. Residues are annotated with their 3-letter amino acid code. Hydrophobic residues are all colored with a green interior, whereas polar residues are colored in light purple. Hydrogen atoms explicitly involved in a hydrogen bond are drawn individually, and oriented toward the residues with which they interact. The interaction of GSH with **(A)** 11KN (NF-κB P65 subunit, NF-κB P50 D subunit, I-κB α **(B)** 3BRV (Inhibitor of nuclear factor kappa-B kinase subunit beta, NF-kappa-B essential modulator) **(C)** 3BRT (Inhibitor of NF-κB kinase subunit β, α and NF-κB essential modulator) **(D)** 1109 (Glycogen synthase kinase 3 β) **(E)** 1L6J (Matrix metalloproteinase-9) **(F)** 3MVM\_a (P38 Alpha Map Kinase complexed with

pyrrolotriazine inhibitor 7V subunit a) (**G**) 3MVM\_b (P38 Alpha Map Kinase complexed with pyrrolotriazine inhibitor 7V subunit b).

**Table 1.** Protein-ligand interaction details

Protein Id	Interaction (D...H-A)	Bond length	Gold score	Binding Energy Kcal/Mol
<b>IκB-NFκB complex (1IKN)</b>	OG(Ser83)...01	2.835	50.42	- 8.65
	N(Glu284)...02	2.559		
	O (Glu284)...02	3.017		
	N (Ser288)...02	2.666		
	N (Glu287)...02	2.755		
	NH1 (Arg246)...04	2.628		
	ND1 (His245)...04	2.700		
	OE1 (Gln249)...05	2.787		
	ND1 (His245)...05	2.528		
<b>NEMO/IKK (3BRV)</b>	OE1 (Gln67)...04	2.986	54.36	- 6.37
	NE1 (Gln67)...05	2.848		
	O (Val709)...N3	2.725		
	OG (Ser68)...S1	2.609		
	OG (Ser68)...03	2.458		
	OG (Ser68)...01	2.761		
	OG (Ser68)...N1	2.963		
	OG (Ser68)...01	2.783		
	OD1 (Asn69)...02	2.646		
<b>NEMO/IKK (α,β) (3BRT)</b>	O (Gln83)...04	3.015	47.86	- 1.36
	O (Gln86)...02	2.900		
	N (Lys90)...02	2.604		
	O (Gln730)...S1	2.494		
	OE1 (Glu89)...S1	2.595		
	OE2 (Glu89)...S1	2.980		
<b>GSK3β (1I09)</b>	O (Cys218)...S1	2.869	49.37	- 9.28
	O (Asp260)...S1	2.777		
	NH1 (Arg223)...03	3.054		
	NH1 (Arg223)...06	2.647		
	NH2 (Arg223)...06	2.933		
	NH1 (Arg223)...06	3.052		
	NH1 (Arg223)...N2	3.078		
	O (Asp260)...01	2.943		
	N (Arg220)...02	2.946		
	OG (Ser215)...N3	2.844		
	O (Ser215)...04	2.879		
	OG (Ser215)...04	2.496		
	O (Lue227)...04	2.375		
<b>MMP9 protein (IL6)</b>	O (Pro415)...01	2.510	54.49	- 5.43
	O (Ala417)...01	2.446		
	O (Met422)...N1	2.548		
	O (Met422)...02	2.838		
	O (Tyr420)...02	2.404		
	OE1 (Glu402)...05	2.416		
	O (Leu397)...S1	3.090		
<b>Positive Control (3mvm_a)</b>	NE(Arg220)...N4	3.080	58.06	- 1.96
	NH2 (Arg237)...N5	2.708		
	O (Val319)...N6	2.658		
<b>Positive Control (3mvm_b)</b>	NE (Arg220)...N4	3.094	60.42	- 3.64
	NH2 (Arg237)...N5	2.453		

**Table 1:** Interaction values in the form of GOLD Score and binding energy Kcal/mol have been enlisted. The binding energy are comparable between -5 to -10. The GOLD score compared with that of the positive control i.e. 3MVM\_a and b indicates probable inhibition of GSH with that of the NF-κB regulators and target MMP9.

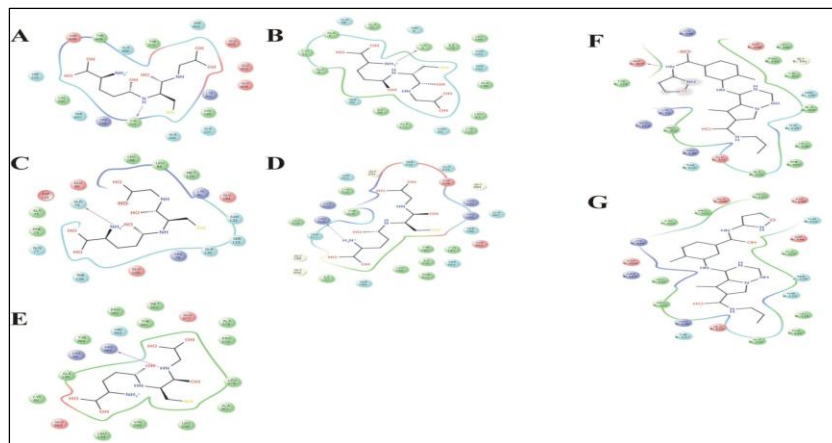


**Fig 2.** (A-E) Visualizations of interaction of GSH with the proteins. (F, G) positive control

Ramachandran plots exhibit no significant changes in the conformation of the docked proteins compared to that of undocked proteins (data not shown). The change may not be necessary since the known inhibitor of P38 MAPK also did not induce change in conformation as evident in Ramachandran plot before and after docking. Thus, molecular docking simulations in both Hex 6.3 and GOLD suite 5.0 reveal significant interactions of the kinases with the GSH molecule. It was interesting to know the presence of thiol group interaction with four out of the five models as shown in Table 1. Probably the thiol interaction is an indicative of favoring “glutathionylation”. It is interesting to know that not only the kinases but even the MMP9 protein has the ability of direct inhibition by excess of GSH. **Fig 3** represents all the three scores from Hex, GOLD and PEARLS in 100% stacked, trend of the percentage. The trend from all the three scores are similar as shown in **fig: 3**.

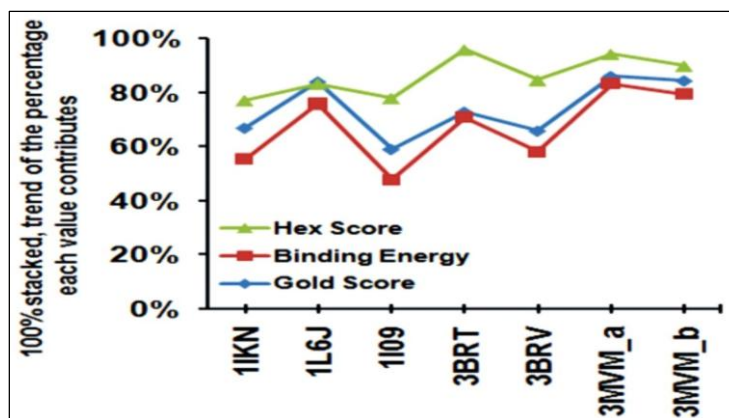


**Fig 3.** The affinity trend as shown by Gold score, Binding Energy and Hex score altogether

**Fig 3:** Representation of all the three scores from Hex, GOLD and PEARLS in 100% stacked, trend of the percentage. The trend from all the three scores are similar. Specifically GOLD (being more accurate) and binding energy scores are found to support the hypothesis at each point.

Specifically GOLD (being more accurate) and binding energy scores give the impression in support of the hypothesis at each point.

GSH inhibits organomercurial activation of pro-MMP-9 by a mechanism that involves protein S-thiolation. Significant inhibition by GSH was noted in the MMP-9 assays. GSH binds at or near the enzyme's active-site Zn<sup>2+</sup> molecule, provided mechanistic insights into how reduced thiols inhibit MMP-9 function. 2.5mM GSH inhibited APMA-induced activation of pro-MMP9 while 2.5mM GSSG did not affect APMA-induced activation of pro-MMP9. GSH addition demonstrated a dose-dependent outcome, with the maximum inhibition detected at the highest (500x) GSH level [23]. This shows why a cancerous cell has an altered redox status mediated by glutathione. Little success can be attributed to the radio-therapeutic approach where MMP9 is inhibited by using MMP9 specific inhibitors (Ad-MMP9) followed by ionizing radiation. This reduces the MMP9 expression followed by decreased phosphorylation of ERK resulting in inhibition of transcriptional activation of NF-κB by ERK, therefore increasing apoptosis in the tumor [24]. The cellular distribution of individual NF-κB—I-κBs appears to be very dynamic and specifically regulated suggesting that their compartmentalization may play a more complex regulatory role than simply shutting down NF-κB induced gene expression [25].

In an important contribution [26] endothelial cells were treated with GSSG (but not GSH) to observe transient block in NF-κB-p65 translocation but independent of IκBα degradation and the effects were comparable to application of 15-deoxy-Δ<sup>12</sup>, 14-prostaglandin J<sub>2</sub> (15 d-PGJ<sub>2</sub>) which also inhibited NF-κB-p65 translocation as a result of Nrf2 mediated increase in GSH which is independent of IκBα degradation. According to a recent report,

P65 translocation have been shown to be inhibited by glutathionylation of P65 induced by mild oxidative stress upon treatment with CO. This phenomenon was reversed upon DTT or BSO treatment [27]. Glutathionylation requires GSSG/GSH ratio to be high. Glutathionylation and de-glutathionylation are enzymatic processes. Our hypothesis is different in a way that we are achieving the same effect without the involvement of enzymes. Perhaps, this strategy is important since one cannot expect the glutathionylation machinery to be intact upon radio therapy for treatment of cancer, besides our aim is to protect the adjacent normal tissues and sensitize the cancerous hypoxic core which is protected by NF- $\kappa$ B signaling pathway from undergoing hypoxic apoptosis [28]. Their results suggest that Gird-dependent protein S-glutathionylation of NF $\kappa$ B-p65 is presumably responsible for NAC-mediated NF- $\kappa$ B inactivation and increased hypoxic apoptosis. But this strategy does not stop nuclear translocation of NF- $\kappa$ B-p65 subunit but check its DNA binding ability; this could be reversible and may offer dire consequences on the other hand. Perhaps it supports our strategy to use reduced glutathione (GSH) directly as it seems that at higher concentrations it can inhibit the kinase activity of the NF- $\kappa$ B activating kinases thereby inhibiting, on the first hand, nuclear translocation of NF- $\kappa$ B-p65 resulting in decrease in the metastatic potential of the cancer cells.

## DISCUSSION

It is noteworthy in a study conducted to demarcate radiation-induced persistent alterations in gene expression in mouse mammary glands two months after radiation exposure [29]; it was observed that exposure to clinical doses escort to long term up-regulation of genes responsible for carcinogenesis, therefore after therapeutic exposure to radiation, breast cancer initiation/progression becomes a challenge to deal with. Furthermore among the up-regulated genes, the Ingenuity Pathway Analysis (IPA) network with highest score has NF- $\kappa$ B as the nodal molecule and qRT-PCR analysis exemplified a 1.65-fold increase in expression of NF- $\kappa$ B in irradiated samples relative to control samples [29]. So, it is principally more important to modulate the messages or the redox state which governs the fate of a cell than just to create lesions on the DNA of a cancer cell. Therefore, we have hypothesized here the strategy to modulate the redox state, to take control of the message delivered by the NF- $\kappa$ B pathway using reduced glutathione and let it release its therapeutic payload thereby limiting metastasis. Both tolerance and effectiveness, however, are important considerations while weighing up potential chemo-preventive compounds. In conclusion, this theory suggests that by virtue of glutathione's redox-modulating, gelatinase-inhibitory and kinase binding properties, an appropriate threshold for GSH concentration have to be determined which exerts the hypothesized function and may, in the near future, represents a promising compound which merit consideration for controlled release, site-directed and chemo-preventive applications.

## ACKNOWLEDGMENT

This work was supported by the then Head of the Department of Biotechnology and Bioinformatics by allowing access to the bioinformatics facility and all the authors are thankful to him.

## AUTHOR'S CONTRIBUTION

NG gave the hypothesis, analyzed the data and prepared the manuscript. BJ and AB contributed in the protein-ligand docking studies.

## CONFLICT OF INTEREST

The authors hereby declare that they do not have any conflict of interest.

## REFERENCES

1. Stamenkovic, I.2000. Matrix metalloproteinases in tumor invasion and metastasis. *Semin Cancer Biol.*, 10:415–433.
2. Galis, Z.S., Asanuma, K., Godin, D. & Meng, X. 1998. N-Acetyl-cysteine decreases the matrix-degrading capacity of macrophage-derived foam cells: new target for antioxidant therapy. *Circulation.* 97:2445–2453 .
3. Oak, M.H., Chataigneau, M., Keravis, T., Chataigneau, T., Beretz, A., Andriantsitohaina, R., Stoclet, J.C., Chang, S.J. & Schini-Kerth, V.B. 2003. Red wine polyphenolic compounds inhibit vascular endothelial growth factor expression in vascular smooth muscle cells by preventing the activation of the p38 mitogen-activated protein kinase pathway. *Arterioscler. Thromb. Vasc. Biol.*, 23:1001–1007 .
4. Oak, MH-E.I., Bedoui, J., Anglard, P. & Schini-Kerth, V.B. 2004. Red wine polyphenolic compounds strongly inhibit pro-matrix metalloproteinase- 2 expression and its activation in response to thrombin via direct inhibition of membrane type 1-matrix metalloproteinase in vascular smooth muscle cells. *Circulation.* 110:1861–1867 .
5. Russell, J.S., Raju, U., Gumin, G.J. et al. 2002. Inhibition of radiation induced nuclear factor- $\kappa$ B activation by an anti-Ras single chain antibody fragment: lack of involvement in radiosensitization. *Cancer Research.* 62:2318-2326 .
6. Takeuchi, K., Motoda, Y. & Ito, F. 2006. Role of transcription factor activator protein 1 (AP-1) in epidermal growth factor-mediated protection against apoptosis induced by a DNA-damaging agent. *FEBS J.*, 273:3743-3755 .

7. Kunigal, S., Joseph, P., Estes, N. & Rao, J.S. 2008. Matrix metalloproteinase-9 Inhibition Down-Regulates Radiation-Induced Nuclear Factor- $\kappa$ B Activity Leading to Apoptosis in Breast Tumors. *Clin Cancer Res.*, 14:3617-3626 .
8. Jung, M. & Dritschilo, A. 2001. NF- $\kappa$ B signaling pathways as a target for human tumor radiosensitization. *Semin Radiat Oncol.*, 11:346-351 .
9. Smirnov, A.S., Ruzov, A.S., Budanov, A.V., Prokhortchouk, A.V., Ivanov, A.V. & Prokhortchouk, E.V. 2001. High Constitutive level of NF- $\kappa$ B is crucial for viability of adeno-carcinoma cells. *Cell Death Differ.* 8:621-630 .
10. Lindholm, P.F., Bub, J., Kaul, S., Shidham, V.B., Kajdacsy, & Balla, A. 2000. The role of constitutive NF- $\kappa$ B activity in PC-3 human prostate cancer cell invasive behavior. *Clin Exp Metastasis.*, 18:471-479 .
11. Giri, D.K. & Aggarwal, B.B. 1998. Constitutive activation of NF- $\kappa$ B causes resistance to apoptosis in human cutaneous T cell lymphoma HuT-78 cells. Autocrine role of tumor necrosis factor and reactive oxygen intermediates. *J Biol Chem.*, 273:14008-14014 .
12. Sato, H. & Seiki, M. 1993. Regulatory mechanism of 92 kDa type IV collagenase gene expression which is associated with invasiveness of tumor cells. *Oncogene*, 8:395-405 .
13. Garg, A. & Aggarwal, B.B. 2002. Nuclear transcription factor- $\kappa$ B as a target for cancer drug development. *Leukemia*. 16:1053-1068 .
14. Cha, H.J., Bae, S.K., Lee, H.Y., Lee, O.H., Sato, H., Seiki, M., Park, B.C. & Kim, K.W. 1996. Anti-invasive activity of ursolic acid correlates with the reduced expression of matrix metalloproteinase-9 (MMP-9) in HT1080 human fibrosarcoma cells. *Cancer Res.*, 56:2281-2284 .
15. Nagakawa, Y., Aoki, T., Kasuya, K., Tsuchida, A. & Koyanagi, Y. 2002. Histologic features of venous invasion, expression of vascular endothelial growth factor and matrix metalloproteinase-2 and matrix metalloproteinase-9, and the relation with liver metastasis in pancreatic cancer. *Pancreas*. 24:169-178 .
16. Murono, S., Yoshizaki, T., Sato, H., Takeshita, H., Furukawa, M. & Pagano, J.S. 2000. Aspirin inhibits tumor cell invasiveness induced by Epstein-Barr virus latent membrane protein 1 through suppression of matrix metalloproteinase-9 expression. *Cancer Res.*, 60:2555-2561 .
17. Banerjee, S., Bueso-Ramos, C. & Aggarwal, B.B. 2002. Suppression of 7, 12- dimethylbenz (a) anthracene-induced mammary carcinogenesis in rats by resveratrol: role of nuclear factor- $\kappa$ B, cyclooxygenase 2, and matrix metalloprotease 9. *Cancer Res.*, 62:4945-4954 .
18. Esther, K., Jordi, R., Pascal, M. & Didier, R. 2004. Comparative evaluation of eight docking tools for docking and virtual screening accuracy. *Protein: Structure, function and bioinformatics*. 57:225-242 .
19. Han, L.Y., Lin, H.H., Li, Z.R., Zheng, C.J., Cao, Z.W., Xie, B. & Chen, Y.Z. 2006. PEARLS: program for energetic analysis of receptor-ligand system. *J Chem INF Model.*, 46:445-450 .
20. Aruoma, O.I. 1999. Antioxidant actions of plant foods: use of oxidative DNA damage as a tool for studying antioxidant efficacy. *Free Rad Res.*, 30:419-427.
21. Kamat, J.P., Ghosh, A. & Devasagayam, T.P. 2000. Vanillin as an antioxidant in rat liver mitochondria: Inhibition of protein oxidation and lipid peroxidation induced by photosensitization. *Mol Cell Biochem*. 209:47-53.
22. Lirdprapamongkol, K., Sakurai, H., Kawasaki, N., Choo, M.K., Saitoh, Y., Aozuka, Y., Singhirunnusorn, P., Ruchirawat, S., Svasti, J. & Saiki, I. 2005. Vanillin suppresses in vitro invasion and in vivo metastasis of mouse breast cancer cells. *Eur J Pharm Sci.*, 25:57-65 .
23. Ping, P., Horan, M., Hille, R., Hemann, C.F., Schwendeman, S.P. & Mallery, S.R. 2006. Reduced nonprotein thiols inhibit activation and function of MMP-9: Implications for chemoprevention. *Free Radic Biol Med.*, 41:1315-1324.
24. Kunigal, S., Lakka, S.S., Joseph, P., Estes, N. & Rao, J.S. 2008. Matrix metalloproteinase-9 Inhibition Down-Regulates Radiation-Induced Nuclear Factor- $\kappa$ B Activity Leading to Apoptosis in Breast Tumors. *Clin Cancer Res.*, 14:3617-3626 .
25. Valovka, T. & Michael, H.O. 2011. p65 controls NF- $\kappa$ B activity by regulating cellular localization of I- $\kappa$ B $\beta$ . *Biochem J.*, 434:253-263 .
26. Yuan-Chun Lin, G.D.H., Chia-Wen Hsieh. & Being-Sun, W. 2012. The glutathionylation of p65 modulates NF- $\kappa$ B activity in 15-deoxy- $\Delta$ 12,14-prostaglandin J2-treated endothelial cells. *Free Rad Biol Med.*, 52:1844-1853.
27. Po-Yen Yeh, C.Y., Chia-Wen Hsieh, Yan-Chang Yang, Po-Min Yang. & Being-Sun Wung. 2014. CO-releasing molecules and increased hemeoxygenase-1 induce protein S glutathionylation to modulate NF- $\kappa$ B activity in endothelial cells. *Free Rad Biol Med*, 70:1-13.
28. Qanungo, S., Starke, D.W., Pai, H.V., Mieval, J.J. & Nieminen, A.L. 2007. Glutathione Supplementation Potentiates Hypoxic Apoptosis by S-Glutathionylation of p65-NF $\kappa$ B. *J Biol Chem.*, 282:18427-18436 .
29. Datta, K., Hyduke, D.R., Suman, S., Moon, B.H., Johnson, M.D. & Fornace, A.J.Jr. 2012. Exposure to ionizing radiation induced persistent gene expression changes in mouse mammary gland. *Rad Oncol.*, 7.